Relating Tensile, Bending, and Shear Test Data of Asphalt Binders to Pavement Performance

J.-S. Chen and C.-J. Tsai

(Submitted 28 April 1998; in revised form 28 May 1998)

Eight different asphalt binders representing a wide range of applications for pavement construction were tested in uniaxial tension, bending, and shear stresses. Theoretical analyses were performed in this study to convert the data from the three engineering tests to stiffness moduli for predicting pavement performance. At low temperatures, high asphalt stiffness may induce pavement thermal cracking; thus, the allowable maximum stiffness was set at 1,000 MPa. At high temperatures, low asphalt stiffness may lead to pavement rutting (ruts in the road); master curves were constructed to rank the potential for rutting in the asphalts. All three viscoelastic functions were shown to be interchangeable within the linear viscoelastic region. When subjected to large deformation in the direct tension test, asphalt binders behaved nonlinear viscoelastic in which the data under bending, shear and tension modes were not comparable. The asphalts were, however, found to exhibit linear viscoelasticity up to the failure point in the steady-state strain region.

Keywords asphalt binders, bending stress, direction tension, pavement performance, shear modulus

1. Introduction

Approximately 100 billion U.S. dollars are spent annually on global pavement construction and maintenance. An estimated 96% of this sum provides flexible pavements made of asphalts and aggregates (Ref 1). Asphalts serving as the primary binder in flexible pavements are considered one of the predominant factors affecting pavement performance. In order to prevent premature pavement failure and to reduce expenditure on maintenance, understanding of the stress-strain behavior of asphalts is necessary. Under the assumption of linear viscoelasticity of asphalts, researchers have developed various models to calculate pavement response and predict pavement performance (Ref 2-6).

For example, van der Poel successfully correlated the stiffness of bitumen obtained at very small strains to two empirical parameters, namely the penetration at 25 °C and the ring and ball softening point (Ref 7). Ever since its publication in 1954, the van der Poel nomograph has been widely used for estimating the mechanical behavior of asphalt binders under various operating conditions.

Because the small-strain behavior of asphalt binders is well studied, traditional approaches toward modeling asphalt binders have retained the assumption of linear viscoelastic behavior. On the application of micromechanical models to predict properties of pavement performance, the linear viscoelasticity of asphalt binders is generally assumed (Ref 8, 9). The hypothesis of asphalts exhibiting linear viscoelastic behavior up to the failure point is, however, not yet validated.

J.-S. Chen and **C.-J. Tsai,** National Cheng-Kung University, Department of Civil Engineering, Tainan 70101, Taiwan, R.O.C. Contact e-mail: jishchen@mail.ncku.edu.tw.

When pavements reach the point of fracture, asphalt binders generally experience great deformation. Nevertheless, asphalt binders undergoing large strains are poorly understood. Devices recently developed from the Strategic Highway Research Program (SHRP) can help researchers determine the fundamental properties of asphalt binders at large strains. The direct tension (DT), the bending beam rheometer (BBR), and the dynamic shear rheometer (DSR) tests can be used to determine the tension, bending, and shear stress of asphalts, respectively. These devices can better measure asphalts subjected to large deformation. However, the relationship of engineering properties among tensile, shear, and bending stresses remains unknown for asphalt binders. To predict pavement performance, it is imperative to evaluate the asphalt binders in the following terms: (a) under what conditions can the linear viscoelasticity be applied and (b) what are the tensile, bending, and shear stresses in relation to each other.

This research is (a) to study the effect of tensile, shear, and bending stresses on pavement performance, (b) to investigate the linear viscoelasticity of asphalts under large deformation, and (c) to propose a suitable procedure to convert tensile, bending, and shear stresses into stiffnesses for comparison. The present work is intended to provide better understanding of the engineering properties of asphalt binder and to help engineers better control pavement performance.

2. Materials and Methods

Three devices were used to study the engineering properties of eight asphalts. These included direct tension, bending beam rheometer, and dynamic shear rheometer devices illustrated in Fig. 1.

2.1 Materials

Eight kinds of asphalt binders (Table 1) were selected for experimental investigation. These asphalts correlate with a

wide range of practical usages for pavements that serve in hot and cold regions. For example, AC-20 grade is most commonly used for paving in northern America, and AC-20 is specified based upon asphalt's viscosity that would be 2000 ± 400 poises at 60 °C. In spite of the same grade, asphalt's properties at other temperatures may be greatly varied under other consistency tests such as softening point and penetration. The conventional tests listed in Table 1 are empirical in nature, and no performance-related properties of asphalt binders can be obtained.

2.2 Direct Tension Test

The DT device (SATEC Systems, Inc., Grove City, PA) measures the tensile properties of asphalt binders. Dogbone shape specimens were cast in a silicone rubber mold, gripped by pins as end pieces, and pulled in tension until rupture occurred. Stress and elongation were measured by a load cell and a laser system respectively and restored as American Standard Code for Information Interchange (ASCII) files for analyses. The tensile strength and strain-to-failure at various temperatures were recorded. Each type of asphalt was tested for four replicates. During the experimental process, test samples were shown to fail in the middle of each specimen and no air bulbs were observed in the sample, indicating that asphalt binders are well prepared and bound to the end pieces.

2.3 Bending Beam Rheometer

The Cannon BBR (Cannon Instrument Corporation State College, PA) was used to measure the flexural creep stiffness of asphalt binders at low temperatures. After being poured into a beam mold, asphalt exposed outside of the mold was trimmed using a hot-knife edge. Caution was exercised to demold the sample and to prevent any damage to the beam. The mold used to produce the beam consisted of aluminum bars and plastic strips. The BBR test was conducted by applying a constant load at the midspan of a small asphalt cement beam that was simply supported. During the test the deflection of the center point of the beam was measured continuously. Each asphalt type with two replicates was tested in three loads: 50, 100, and 200 grams.

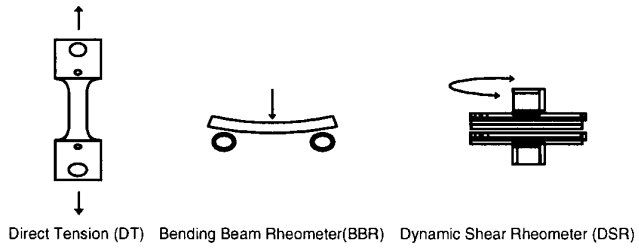

Fig. 1 Schematic drawing of devices used in this study

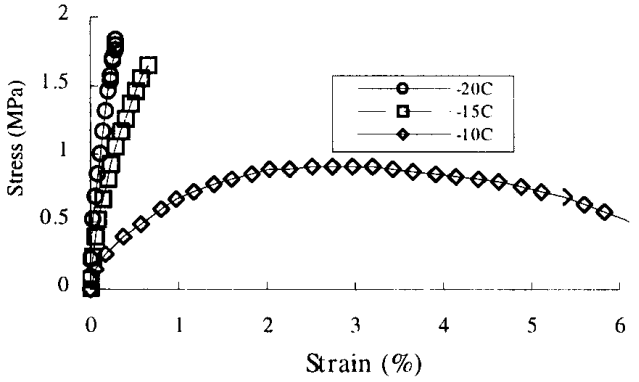

Fig. 2 Stress-strain curves for asphalt specimen A under direct tension at constant strain rate 1 mm/min

2.4 Dynamic Shear Rheometer

The DSR model RMS-803 (Rheometric, Inc., Piscataway, NJ) was used to measure the shear moduli of the asphalt binder in the sinusoidal loading mode under different temperatures. The rectangular torsion bar and parallel plates were used to test samples. Torsion rectangular specimens were prepared in molds made of brass stock and covered with cellophane to aid in demolding the asphalt bar, while asphalts in the parallel plates were carefully trimmed. Two measurements for each asphalt were obtained over a range of frequencies to determine the time dependency of the asphalt binder. Data acquisition systems were included in a commercial stress rheometer; users of these devices will not normally need to be concerned with the details of data acquisition.

3. Tensile Properties of Asphalt Binders

Typical results of stress versus strain (shown in Fig. 2) indicate that for each temperature, the stress increases with the strain, up to a peak point. Asphalts tested at low temperatures tended to exhibit fracture behavior in the brittle region and fail at low strains. On the other hand, the ductile behavior at relatively high temperatures extended asphalts to large deformation and may continuously stretch them into thin threads.

Table 1 Conventional properties of asphalt binders employed in experiments

Specimen	Grade	Ring and ball softening point, °C	Penetration at 25 °C, 100 g, 5 s, 0.1 mm
A	AC-5	44	160
B	AC-10	48	98
C	AC-5	43	133
D	AC-10	48	135
E	AC-20	50	55
F	AC-20	49	53
G	AC-30	49	70
H	AC-40	52	64

Specimen	Viscosity at 135 °C, centistoke	Ductility at 4 °C, 5 cm/min, cm	Penetration at 4 °C, 100 g, 5 s, 0.1 mm
A	283	150+	15
B	289	40	6
C	179	137	7
D	309	150+	9
E	327	8	0
F	243	0	2
G	562	28	2
H	569	5	4

Asphalt tensile strength at –10 °C decreased as a result of necking in the middle of the samples. The peak stress, peak strain, and failure energy of asphalt binders are listed in Table 2. Failure energy was computed by numerically integrating the stress-strain curve up to the point of instability. As temperature increased, the tensile strength of asphalt binders decreased. The peak strain, however, elongated, and the failure energy increased. Asphalts with low peak strain and failure energy may be subjected to low-temperature thermal cracking. Relatively brittle asphalt binders were samples B and G in Table 2, both of which may cause premature pavement cracking at low temperatures.

3.1 Steady-State Behavior under Direct Tension

In analyzing the stress-strain behavior for time and temperature dependent materials such as asphalt binders, the strain at the maximum observed load is defined as the steady-state strain corresponding to a particular temperature. It can be seen in Fig. 3 that at a constant strain rate, the steady-state strain increases with time until fracture occurs. The curve in Fig. 3 comprises three parts: the primary (I), secondary (II), and tertiary (III) regions. The primary region is related to the short period of time when asphalt samples adjusted themselves in the DT as loads were applied. The secondary strain is taken as the steady-state response of asphalt binders when subject to the applied stress. The tertiary region appeared to be within a limited range at temperatures less than –15 °C, but it expanded to a much larger scale when temperatures were higher than –10 °C. Paving technologists have used the limiting stiffness concept to predict low-temperature thermal shrinkage cracking since the early 1960s (Ref 10-12). Stiffness needs to be calculated to verify the concept. Procedures to be described were developed to compute stiffness from the DT.

Table 2 Tensile properties

Specimen	AC temperature, °C	Peak stress, MPa	Peak strain, %	Failure energy, MPa
A	–20	1.78	0.67	0.005
	–15	1.62	0.84	0.075
	–10	1.01	9.9	0.111
B	–20	1.93	0.36	0.003
	–15	1.40	2.26	0.033
	–10	1.41	7.00	0.081
C	–20	2.86	0.55	0.008
	–15	2.28	3.69	0.073
	–10	1.62	7.13	0.095
D	–20	1.93	1.43	0.017
	–15	1.85	3.54	0.046
	–10	1.21	7.62	0.075
E	–20	1.72	0.96	0.010
	–15	1.57	3.33	0.037
	–10	1.24	5.35	0.052
F	–20	2.55	0.72	0.011
	–15	2.06	4.67	0.077
	–10	0.98	7.33	0.062
G	–20	1.98	0.42	0.003
	–15	1.51	6.74	0.090
	–10	1.06	10.06	0.090
H	–20	3.84	1.44	0.034
	–15	3.80	4.48	0.128
	–10	2.34	5.62	0.130

3.2 Stiffness from Direct Tension Test

The term *stiffness* was originally coined by van der Poel (1954) and is widely used among asphalt technologists for predicting pavement performance (Ref 7). When a strain ε is applied to a sample during a time interval t, and the time-dependent stress during the time increment is given by:

$$\sigma(t) = E(t) \cdot \varepsilon \quad \text{(Eq 1)}$$

then the response to any arbitrary strain history in a simple tension can be represented by the integral equation:

$$\sigma(t) = \int_0^t E(t-u) \cdot \frac{d\varepsilon}{du}\, du \quad \text{(Eq 2)}$$

where u is the variable of integration. When a specimen is elongated at a constant strain rate, $\bar{\varepsilon}$, the previous equation becomes:

$$\sigma(t) = \bar{\varepsilon} \cdot \int_0^t E(t-u)du \quad \text{(Eq 3)}$$

By replacing $\bar{\varepsilon}$ with $\varepsilon(t)/t$, the secant modulus, $F(t)$, at any arbitrary strain is defined as follows:

$$F(t) = \frac{\sigma(t)}{\varepsilon(t)} = \frac{1}{t} \cdot \int_0^t E(t-u)du \quad \text{(Eq 4)}$$

After multiplying by t on both sides of this equation, the following equation is obtained:

$$F(t) \cdot t = \int_0^t E(t-u)du \quad \text{(Eq 5)}$$

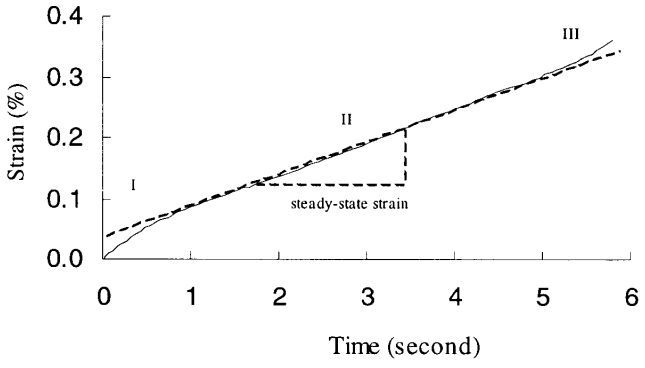

Fig. 3 Strain-loading time curve for asphalt C under direct tension at –15 °C

After differentiating the above equation with respect to time, the stiffness, $E(t)$, can be expressed as:

$$E(t) = F(t) + t \cdot \frac{dF(t)}{dt} \quad \text{(Eq 6)}$$

Based upon calculus, $dt = t \cdot d\log t$ and $dF(t) = F(t) \cdot d\log F(t)$, this equation can be rewritten in the form of:

$$E(t) = F(t) \cdot \left[1 + \frac{d\log F(t)}{d\log t}\right] \quad \text{(Eq 7)}$$

For deformation in simple extension at a constant rate of strain, this study proposed that the stiffness of asphalts tested under direct tension be computed by Eq 7. Figure 4 demonstrates an example of using the secant modulus to obtain the relaxation modulus.

Studies indicated that pavements may crack at an asphalt binder's stiffness greater than 1,000 MPa at 1800 second loading time when temperatures at –15 °C (Ref 10-11). The limiting stiffness in Table 3 indicates that asphalts B, E, F, and G are brittle and may suffer low-temperature cracking. It should be noted that the limiting stiffnesses obtained in Table 3 are within the steady state.

4. Bending Properties of Asphalt Binders

The engineering properties obtained from the BBR test are in a form of creep compliance. The bending properties of asphalt binders can be converted to stiffnesses so that engineers can compare both BBR and DT stiffnesses on the same basis.

Table 3 Limiting stiffness

Asphalt specimen	Limiting stiffness, MPa
A	136
B	1378
C	715
D	516
E	1123
F	1049
G	1431
H	817

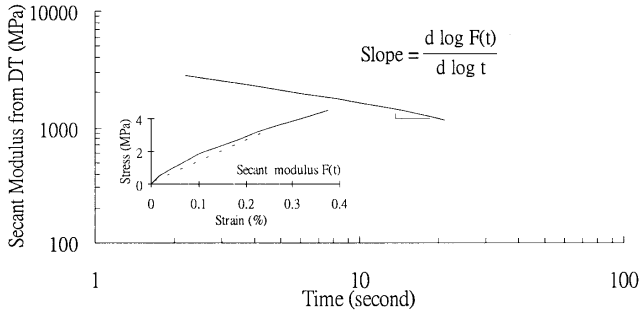

Fig. 4 Example of relaxation modulus derived

Since both tests were conducted at low temperatures and were related to low-temperature pavement cracking, the implication of the binding properties to pavement performance was similar to that of tensile properties. Large deformation observed in the DT, however, needs to be checked if asphalt is to be kept within the linear viscoelastic region. Two checks on the linear viscoelasticity of asphalt binders were performed by the BBR: applying the Boltzmann superposition principle and demonstrating the stress-independence of asphalts.

4.1 Stiffness from BBR

Several approximate relations for interrelating creep compliance, $J(t)$, and stiffness, $E(t)$, have been presented by different researchers (Ref 13, 14). These equations are, however, empirical in nature and are valid only for limited portions of the relaxation spectrum. For these reasons, they are not appropriate for the asphalts.

From a theoretical viewpoint, the interrelation between stiffness and creep response in the time domain can be represented by a convolution integral:

$$\int_0^t E(t-u) \cdot J(u)du = \int_0^t E(u) \cdot J(t-u)du = t \quad \text{(Eq 8)}$$

in which the letter u is the dummy variable in the integration.

An algorithm was developed in this study to solve the convolution integral. The interval of integration was divided into small intervals. A recursion relation was set up from which stiffness eventually was shown as a discrete set of values. If the creep compliance, $J(t)$, is represented in terms of a set of n values, $J(t_i)$, the recursion result for stiffness, $E(t_n)$, is given by:

$$E(t_n) = -E(t_{n-1}) + \frac{4_{t_n} - \sum_{i=1}^{i=n-1} [E(t_i) + E(t_i - 1)] + [J(t_n - t_i) + J(t_n - t_i - 1)](t_i - t_i - 1)}{[J_g + J(t_n - t_n - 1)](t_n - t_n - 1)} \quad \text{(Eq 9)}$$

with

$$E(t_1) = \frac{3 - [J_g/J_{(t_1)}]}{J_g + J_{(t_1)}} \quad \text{(Eq 10)}$$

as the starting value in which J_g is the glassy compliance. The procedure for calculating the stiffness from BBR can be easily performed by a spreadsheet software program. Comparisons between BBR and DT stiffnesses are discussed later.

4.2 Boltzmann Superposition Principle

The Boltzmann superposition principle states that the behavior of a linear viscoelastic material at any time is the linear sum of what happened before (Ref 15, 16). Stepwise loading

was used in this study to verify the Boltzmann superposition principle. The one-step superposition is shown in Fig. 5. A constant stress σ_1 is applied at $t = t_1$, which produces a strain $\varepsilon(t) = \sigma_1/S(t - t_1)$. At $t = t_2$ an additional stress σ_2 is applied, and for $t > t_2$ induced strain is proportional to σ_2 if asphalt is within the linear viscoelasticity. In other words, the additional strain produced by adding σ_2 at t_2 is the same as the strain that would have occurred under σ_2 with no previous loading history. The total strain $\varepsilon(t)$ for $t > t_2$ is determined as follows:

$$\varepsilon(t) = \frac{\sigma_1}{S(t - t_1)} + \frac{\sigma_2}{S(t - t_2)} \quad \text{(Eq 11)}$$

A constant load of 50 g was first applied to the beam, and a creep curve, ε_{50g}, was obtained accordingly. To impose the one-step loading, a 50 g dead load was applied on the sample initially, and another 50 g dead load was added after approximately 120 s. Typical results of loading time plotted against strain at –15 °C were shown in Fig. 5. The strain induced by the added 50 g dead load can be calculated by adding the strain of ε_{50g} after 120 s to the strain of ε_{50g}. The superposition of these two portions of the ε_{50g} curve on the measured curve is shown in Fig. 5. This figure indicates that the calculated data were well matched with the experimental values. Similar results were also observed for other asphalts.

A two-step superposition was further employed. The whole strain, $\varepsilon(t)$, under a two-step superposition is formulated as follows:

$$\varepsilon(t) = \frac{\sigma_1}{S(t - t_1)} + \frac{\sigma_2}{S(t - t_2)} + \frac{\sigma_3}{S(t - t_3)} \quad \text{(Eq 12)}$$

The calculated values are well matched with the experimental data as shown in Fig. 6. All other asphalts also showed similar results that there is a correlation between experimental data and calculated values. This correlation implies that the Boltzmann superposition principle is applicable to the asphalts.

For linear viscoelastic materials, the strain at any given time depends on the previous loading history. This is quite different from what happens in an elastic material, which has a strain that depends solely on the stress acting at that time. The strain of linear viscoelastic materials at time t is, then, the sum of the strain caused by all the steps that have taken place at any time less than t. It was shown in the present study that the strain of asphalts within the region of linear behavior can be generalized for a sequence of finite stress changes σ_i, applied at a time t_i. The equation is expressed as follows:

$$\varepsilon(t) = \sum_{i=1}^{i=n} \frac{\sigma_i}{S(t - t_i)} \quad \text{(Eq 13)}$$

4.3 Stress Independence

The second check for the linear viscoelasticity was to demonstrate that the stiffness of the asphalts is independent of the magnitude of applied loads and that the stiffness is only time and temperature dependent. Three different loads, that is, 50, 100, and 200 g, were applied to the asphalt beams in this study. References were made to the plain asphalt and asphalt data in

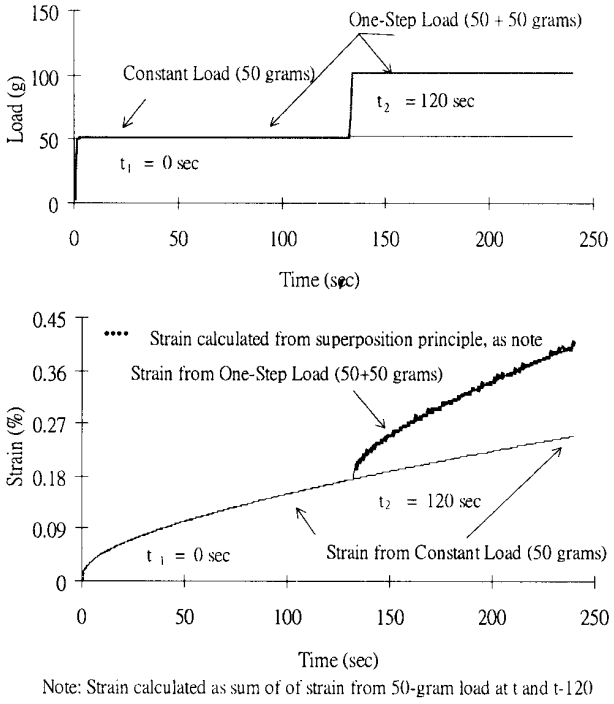

Note: Strain calculated as sum of of strain from 50-gram load at t and t-120

Fig. 5 One-step loading for asphalt F at –15 °C

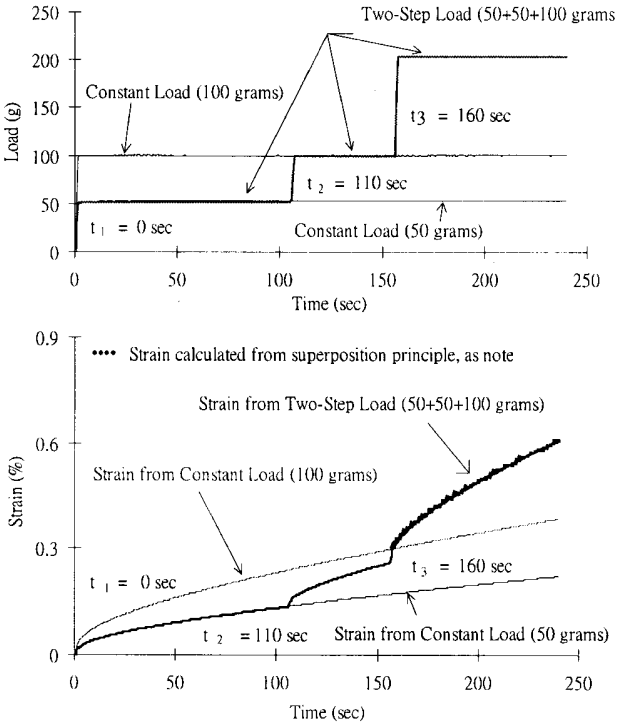

Note: Strain calculated as sum of strain form 50-gram load at t seconds, strain form 50-gram laod at t-100 seconds, and strain from 100-gram at t-160 second

Fig. 6 Two-step loading for asphalt D at –10 °C

Fig. 7. All the data were well lined up the regression line for each free asphalt volume, and there was little difference in the stiffness values under these three loads. The asphalts were shown to be stress-independent materials in the region of testing. Please note that asphalts B, F, and G are relatively stiff compared to the others, and this observation supports previous discussions. At low temperatures stiff asphalts may induce thermal cracking.

It has been confirmed that the Boltzmann superposition principle is applicable to asphalt binders and that asphalts are stress independent. Two checks on the linear viscoelasticity have been satisfied. Therefore, it is concluded that the asphalt is a linear viscoelastic material in the region tested.

5. Shear Properties of Asphalt Binders

The shear moduli, $G(t)$, obtained from the DSR are traditionally converted to stiffnesses by the following equation:

$$E(t) = 3G(t) \quad \text{(Eq 14)}$$

The stiffnesses at different temperatures can be combined into a single master curve using the time-temperature superposition. Through the construction of stiffness master curves, the effect of loading time and temperature on the linear viscoelastic properties of asphalts can be characterized. In constructing the master curves for the asphalts tested, the dynamic mechanical data were shifted on the basis of the loading times. For clarity only four asphalts are shown in Fig. 8. This resulted in fairly smooth viscoelastic functions as shown in Fig. 8. Asphalts are demonstrated to be thermorheological simple materials because the time-temperature superposition is valid for asphalt cements.

At very short loading times, the stiffnesses reach the glassy region at about 3 GPa as shown in Fig. 8. The 3 GPa represents the rigidity of the carbon hydrogen bonds as the asphalts reach their minimum thermodynamic equilibrium volume. At very long loading time, the log-log plot of stiffness versus time approaches a slope of 1 to 1, indicating that viscous flow exists and asphalts behave as a Newtonian fluid. In the intermediate region, centered around the intersection of the glassy and viscous asymptotes, most of the deformation will be of the delayed elastic type. According to the time-temperature principle, the long loading time can be an indicator of asphalts being treated in high temperatures. As shown in Fig. 8, the asphalt resistance of rutting will be specimen G>E>C>D; however, asphalt G may be too brittle to be used at low temperatures, as discussed in the DT test.

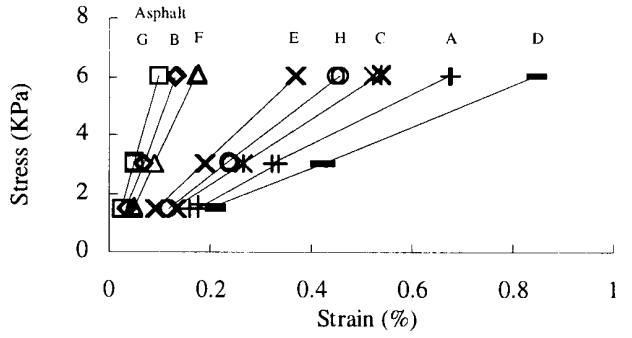

Fig. 7 Stress independence of asphalt binders at –10 °C under bending beam rheometer testing

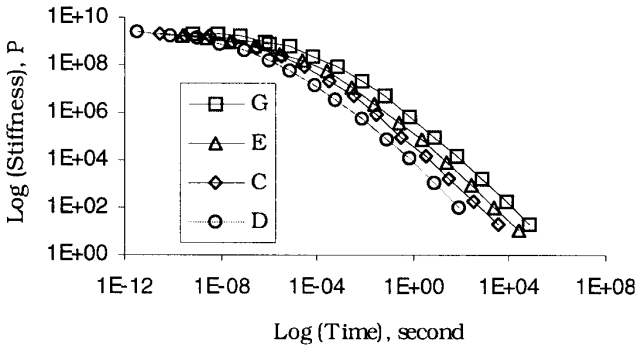

Fig. 8 Master curves constructed from dynamic shear rheometer testing

6. Comparison of Stiffnesses Obtained from DT, BBR, and DSR Tests

To verify that asphalts exhibit linear viscoelastic behavior up to the failure point in the brittle region, the stiffnesses obtained from the DT, BBR, and DSR are compared. The linear viscoelastic behavior of asphalts has been demonstrated by using the BBR and DSR devices, and stiffnesses from both devices were comparable as shown in Fig. 9. The present study thus was to compare the stiffnesses from DT with ones from BBR. If the stiffnesses from DT and BBR tests are comparable at any given loading time and temperature, it can be concluded that the behavior of asphalts is within the linear viscoelastic region under direct tension. On the other hand, if the stiffnesses from the tests are different, it is indicated that the asphalt behavior in the DT is not linear.

The stiffnesses from the DT and BBR were plotted in Fig. 10 and 11 representing test temperatures at –15 °C and –10 °C, respectively. As shown in Fig. 10, the BBR and DT stiffnesses were all on the equality line for asphalts tested at –15 °C, over the range of loading times where samples remained in the

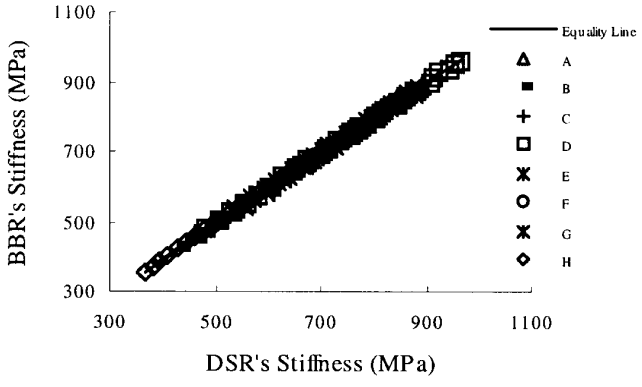

Fig. 9 Comparison of bending beam rheometer and dynamic shear rheometer stiffness at –10 °C

brittle region. Similar trends were also observed at –20 °C. This equality implied that asphalts exhibit linear viscoelastic behavior up to the failure point at these two temperatures. The various representations of viscoelastic behaviors such as bending, tension, and shear thus can be transformed to each other, if there is a linear relationship between stress and strain.

At –10 °C the stiffnesses scattered around the equality line as indicated (Fig. 11). It suggested that the linear viscoelasticity of asphalts is not valid at –10 °C under DT. The observation illustrates that asphalts exhibit linear viscoelastic behavior up to the failure point within the steady-state strain stage. When there is a relatively large deformation, that is, in the tertiary range, asphalts tend to be nonlinear. Thus, the micromechanic model proposed by other researchers (Ref 2-6, 17) based on the assumption of linear viscoelasticity need to be modified for the nonlinear behavior of asphalt binders.

7. Conclusions

The tensile, bending, and shear behavior of asphalt binders were investigated by the direct tension (DT) test, the bending beam rheometer (BBR), and the dynamic shear rheometer (DSR), respectively. DT data can be adequately transformed to stiffnesses by the procedure developed in this study. The numerical solution of the convolution theory was developed to successfully convert BBR's creep compliances to stiffness for asphalts. These three responses were shown to be interchangeable within the linear viscoelastic region. The linear viscoelasticity of asphalt has been maintained up to failure points in the steady state of the direct tension test. Pavement performance can be predicted when asphalts are within the linear viscoelastic range. However, the linear viscoelasticity was not valid when asphalts were subjected to large deformation. The stiffnesses become nonlinear in the tertiary region. This observation implies that extreme care should be taken in the use of micromechanical models when asphalts reach the nonlinear region.

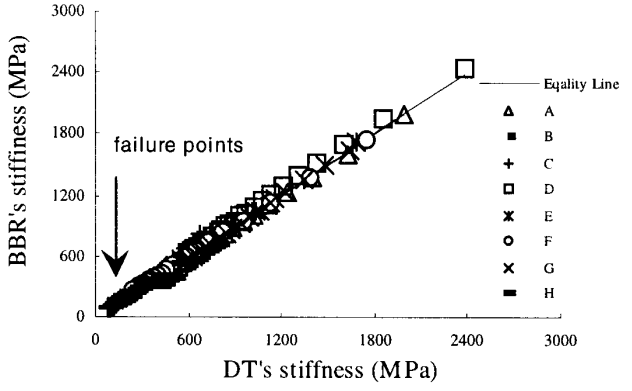

Fig. 10 Comparison of stiffnesses at –15 °C

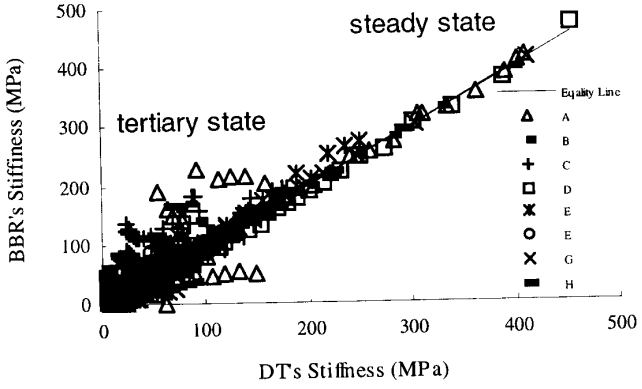

Fig. 11 Comparison of stiffnesses at –10 °C

Acknowledgment

The authors thank the National Science Council for sponsoring research project NSC87-2211-E006-043, which made completion of this article possible.

References

1. Highway Construction and Maintenance, *World Highway,* Nov/Dec 1994, p 65-83
2. C. van der Poel, *Time and Temperature Effects on the Deformation of Asphaltic Bitumens and Bitumen-Mineral Mixtures,* Society of Petroleum Engineers, AIME, 1955, p 47-53
3. E.H. Chipperfield and T.R. Welch, Studies on the Relationships Between the Properties of Road Bitumens and Their Service Performance, *Proc. AAPT,* Vol 36, 1967, p 421-488
4. P.S. Kandhal and M.E. Wenger, Asphalt Properties in Relation to Pavement Performance, *Trans. Res. Rec. 544,* 1977, p 1-13
5. W.B. Buttlar and R. Roque, Evaluation of Empirical and Theoretical Models to Determine Asphalt Mixture Stiffness at Low Temperatures, *Proc. AAPT,* Vol 65, 1996, p 99-141
6. D.A. Anderson, D.W. Christensen, H.U. Bahia, R. Dongre, M.G. Sharma, C.E. Antle, and C.E.J. Button, "Binder Characterization and Evaluation, Vol. III, Physical Characterization," Strategic Highway Research Program Report, SHRP A-369, Washington, D.C., 1994
7. C. van der Poel, A General System Describing the Visco-Elastic Properties of Bitumen and Its Relation to Routine Test Data, *J. Appl. Chem.,* Vol 4, 1954, p 221-236
8. S.H Alavi and C.L. Monismith, Time and Temperature Dependent Properties of Asphalt Concrete Mixes Tested as Hollow Cylinders and Subjected to Dynamic Axial and Shear Loads, *Proc. AAPT,* Vol 63, 1994, p 152-181
9. W.J. Gaw, Measurement and Prediction of Asphalt Stiffnesses and Their Use in Developing Specifications to Control Low-Temperature Pavement Transverse Cracking, STP 629, ASTM, 1997, p 39-45
10. H.J. Fromm and W.A. Phang, Temperature Susceptibility Control in Asphalt Cement Specifications, *HRB 350,* 1971, p 65-79
11. P.S. Kandhal, Evaluation of Low Temperature Pavement Cracking on Elk County Research Project, *Trans. Res. Rec. 777,* 1971, p 39-49
12. E.E. Redshaw, Asphalt Specifications in British Columbia for Low Temperature Performance, *Proc. AAPT,* Vol 41, 1972, p 87-101
13. E.J. Dickinson and H.P. Witt, The Dynamic Shear Modulus of Paving Asphalts as a Function of Frequency, *Trans. Soc. of Rheol.,* Vol 18 (No. 4), 1974, p 591-606
14. G.R. Dobson, On the Development of Rational Specifications for the Rheological Properties of Bitumens, *J. Inst. Pet.,* Vol 58 (No. 559), 1972, p 14-24
15. W. Flugge, *Viscoelasticity,* 2nd ed., Springer-Verlag, Berlin, 1975
16. N.W. Tschoegl, *The Phenomenological Theory of Linear Viscoelastic Behavior,* Spring-Verlag, Berlin Heidelberg, 1989
17. R.A. Schapery, Viscoelastic Behavior and Analysis of Composite Materials, *Composite Materials,* Vol 2, G.P. Sendeckyj, Ed., Academic Press, 1974, p 84-168